



Repair of Radiation-Induced DNA Double-Strand Breaks Is Dependent upon Radiation Quality and the Structural Complexity of Double-Strand Breaks

Author(s): Elzbieta Pastwa, Ronald D. Neumann, Katherina Mezhevaya and Thomas A. Winters

Source: *Radiation Research*, Vol. 159, No. 2 (Feb., 2003), pp. 251-261

Published by: [Radiation Research Society](#)

Stable URL: <http://www.jstor.org/stable/3580834>

Accessed: 20/06/2014 18:53

Your use of the JSTOR archive indicates your acceptance of the Terms & Conditions of Use, available at <http://www.jstor.org/page/info/about/policies/terms.jsp>

JSTOR is a not-for-profit service that helps scholars, researchers, and students discover, use, and build upon a wide range of content in a trusted digital archive. We use information technology and tools to increase productivity and facilitate new forms of scholarship. For more information about JSTOR, please contact support@jstor.org.



Radiation Research Society is collaborating with JSTOR to digitize, preserve and extend access to *Radiation Research*.

<http://www.jstor.org>

Repair of Radiation-Induced DNA Double-Strand Breaks is Dependent upon Radiation Quality and the Structural Complexity of Double-Strand Breaks

Elzbieta Pastwa,^{a,b} Ronald D. Neumann,^a Katherina Mezhevaya^{a,1} and Thomas A. Winters^{a,2}

^a Nuclear Medicine Department, Warren Grant Magnuson Clinical Center, National Institutes of Health, Bethesda, Maryland 20892; and

^b Department of General Chemistry, Institute of Physiology and Biochemistry, Medical University of Lodz, Poland

Pastwa, E., Neumann, R. D., Mezhevaya, K. and Winters, T. A. Repair of Radiation-Induced DNA Double-Strand Breaks is Dependent upon Radiation Quality and the Structural Complexity of Double-Strand Breaks. *Radiat. Res.* 159, 251–261 (2003).

Mammalian cells primarily repair DSBs by nonhomologous end joining (NHEJ). To assess the ability of human cells to mediate end joining of complex DSBs such as those produced by chemicals, oxidative events, or high- and low-LET radiation, we employed an *in vitro* double-strand break repair assay using plasmid DNA linearized by these various agents. We found that human HeLa cell extracts support end joining of complex DSBs and form multimeric plasmid products from substrates produced by the radiomimetic drug bleomycin, ⁶⁰Co γ rays, and the effects of ¹²⁵I decay in DNA. End joining was found to be dependent on the type of DSB-damaging agent, and it decreased as the cytotoxicity of the DSB-inducing agent increased. In addition to the inhibitory effects of DSB end-group structures on repair, NHEJ was found to be strongly inhibited by lesions proximal to DSB ends. The initial repair rate for complex non-ligatable bleomycin-induced DSBs was sixfold less than that of similarly configured (blunt-ended) but less complex (ligatable) restriction enzyme-induced DSBs. Repair of DSBs produced by γ rays was 15-fold less efficient than repair of restriction enzyme-induced DSBs. Repair of the DSBs produced by ¹²⁵I was near the lower limit of detection in our assay and was at least twofold lower than that of γ -ray-induced DSBs. In addition, DSB ends produced by ¹²⁵I were shown to be blocked by 3'-nucleotide fragments: the removal of these by *E. coli* endonuclease IV permitted ligation. © 2003 by Radiation Research Society

INTRODUCTION

DNA double-strand breaks (DSBs) are produced continuously in living organisms as a consequence of oxidative metabolism and exposure to external DNA-damaging

agents such as ionizing radiation or chemicals (1–4). These breaks can have serious consequences, such as chromosomal aberrations, increased genetic instability, carcinogenesis and cytotoxicity (5, 6). Mammalian cells repair DSBs primarily by nonhomologous end joining (NHEJ) (7). The chemical and physical structure of the DSB end group is an important consideration when investigating NHEJ because it may directly affect the pathway's ability to repair a break.

Although the term DSB is descriptive of the physical state of the DNA, it fails to convey the range of complexity existing at most naturally occurring DSB lesions. In addition to a physical discontinuity, most naturally occurring DSBs contain nucleotide fragments at the strand break ends. In the case of most oxidative processes, including low-LET ionizing radiation, these fragments primarily consist of phosphate or phosphoglycolate groups at the 3' ends of the break (8–10). Strand break ends blocked by fragmented nucleotides are not the extent of the lesion complexity produced at DSBs. In addition to blocked ends, nucleotides proximal to the break site may also become damaged in one or both strands and at either or both sides of the discontinuity. Such lesions are referred to as clustered or multiply damaged sites (MDS) (11–13).

Metabolic oxidative processes might occasionally produce these very complex lesions, but they are much more common as a result of exposure to densely ionizing DNA-damaging agents like ionizing radiation (14–16). Consistent with this is an expectation of an increasing yield of MDS with increasing LET of an incident radiation (17).

Data presented in this report are in agreement with this expectation and indicate that as the structural complexity of DSBs increases, repair by NHEJ becomes severely inhibited. To assess repair of DSBs with increasingly complex structures, we employed an *in vitro* DSB repair assay that allowed us to measure DSB repair at lesions produced by DNA-damaging agents ranging from restriction enzymes to site-specific ¹²⁵I decay (18). We found that, in addition to strand break ends, a major inhibitor of NHEJ is damage proximal to the DSB end. Damage in the form of single-

¹ Current address: Fidelity Systems, Inc., Gaithersburg, MD, 20879.

² To whom correspondence should be addressed. Nuclear Medicine Department, Warren Grant Magnuson Clinical Center, National Institutes of Health, Bethesda, MD 20892; e-mail: twinters@mail.cc.nih.gov.

strand breaks or base damage upstream of a ligatable restriction enzyme-induced DSB was found to be highly inhibitory to NHEJ, but these lesions did not affect the ability of T4 DNA ligase to join the ligatable ends.

In addition to assessing DSB repair, we determined several structural characteristics for site specific ^{125}I -induced DSBs, including the presence of nucleotide fragments at the 3' ends of the break.

MATERIALS AND METHODS

Materials

Dulbecco's modified Eagle's medium (DMEM), fetal bovine serum, nonessential amino acids (10 mM), glutamine (100 mM), penicillin/streptomycin (10,000 U/ml), *S. cerevisiae* tRNA, and T4 DNA ligase (1 U/ μl) were purchased from Life Technologies (Gaithersburg, MD). Bleomycin and phenylmethylsulfonyl fluoride (PMSF) were obtained from Sigma (St. Louis, MO). Endonuclease IV (10 U/ μl) was purchased from Trevigen (Gaithersburg, MD). *StuI* (10,000 U/ml) was purchased from New England Biolabs (Beverly, MA). *Vi*stra Green was obtained from Amersham Pharmacia Biotech (Piscataway, NJ).

Protease inhibitors (leupeptin, bestatin, pepstatin and pefablock) were purchased from Boehringer Mannheim (Indianapolis, IN) and aprotinin was from ICN Biomedicals Inc. (Aurora, OH). Automated oligonucleotide synthesis reagents were obtained from Glenn Research (Sterling, VA). ^{125}I -dCTP (81.4 TBq/mmol) was purchased from New England Nuclear (Boston, MA). Plasmid pSP189 and pTC27 were generous gifts from Dr. Michael Seidman (National Institute of Aging, Baltimore, MD).

DNA

Treatment with *StuI*. DNA containing DSBs with ligatable (3'-OH and 5'- PO_4) blunt ends was produced by complete digestion of pSP189 with *StuI* restriction endonuclease. Protein was removed and purified linear plasmid was recovered in TE buffer, pH 8.0, using a Qiagen (Valencia, CA) PCR cleanup kit according to the manufacturer's instructions.

Treatment with bleomycin. Linear DNA containing DSBs with unligatable 3'-phosphoglycolate (PG)-blocked ends was prepared by treating supercoiled pSP189 plasmid DNA with bleomycin. Plasmid DNA was treated as described previously under conditions demonstrated to produce strand breaks exclusively (19). Briefly, DNA at 150 $\mu\text{g/ml}$ in 12.5 mM Tris-HCl, pH 8.0, 300 mM sucrose, 0.0188% Triton X-100, 1.25 mM EDTA, 5 mM MgCl_2 , 7.5 mM β -mercaptoethanol and 250 $\mu\text{g/ml}$ heat-inactivated BSA was treated with bleomycin (0.5 $\mu\text{g/ml}$) at 37°C for 20 min in the presence of 100 μM ferrous ammonium sulfate. The drug was removed by ethanol precipitation and linearized DNA was band isolated and recovered after 1% agarose gel electrophoresis as described previously (20).

^{60}Co γ irradiation. Supercoiled pSP189 plasmid DNA (0.5 $\mu\text{g}/\mu\text{l}$) was irradiated in 50 mM sodium phosphate, pH 7.2, at a range of doses between 0–100 Gy. The dose rate of the irradiator was 1.4 Gy/min. Damaged DNA with a yield of linear DNA similar to that obtained with bleomycin was identified, and the linear DNA was band purified for use in end-joining assays.

Site-Specific Auger Effect-Induced Double-Strand Breaks

Oligonucleotides were synthesized on an Applied Biosystems 394 DNA/RNA synthesizer and band purified from denaturing 20% PAGE. The TC1 27 mer TFO (5'-TCTTTTCTTTCTTTTCTTTTTC-3') labeled with ^{125}I -dCTP at position 27 was constructed by primer extension (21). The 26 mer tc1-primer (5'-TCTTTTCTTTCTTTTCTTTCTTTTTC-3') and the biotinylated 39 mer tc1-template (5'-CCCGAAAAAAGAAGAAAAGAAAGAAAAAGACCCCC-CCCB-3') were an-

nealed (50 mM Tris-HCl, pH 8.0, 10 mM MgCl_2 , 50 mM NaCl) and the primer was extended with 3'-5' exonuclease- Klenow fragment in the presence of ^{125}I -dCTP (81.4 TBq/mmol; primer:template ratio 2:1). The ^{125}I -labeled TC1 27 mer was isolated by heat denaturation of the duplex extension products after binding to streptavidin-labeled magnetic Dynabeads (Dyna, Oslo, Norway). Dynabead-bound template oligonucleotides were separated from the mixture in an ice-cold magnet, and unincorporated nucleotides were removed from the supernatant containing ^{125}I -TC1 by Sephadex G-50 spin column chromatography.

Auger effect damage induced by ^{125}I decay was targeted to pTC27 by the ^{125}I -labeled TC1 27 mer TFO targeted to the polypurine/polypyrimidine TFO binding site engineered into pTC27 immediately upstream of the *SupF* gene. The TFO contains a ^{125}I -dCTP residue at position 27. Upon binding to pTC27, the TFO positions ^{125}I -dCTP one-nucleotide upstream from the 5'-end of the pTC27 *SupF* gene (see Fig. 4A and B). Unbound TFO was removed from the mixture by CL-4B sepharose chromatography and the TFO-bound DNA was stored at -80°C to accumulate damage. TFO-mediated site-specific DSB induction was demonstrated by the production of two appropriate-sized fragments after cleavage of DNA damage products with the single site cutter *Pf*MI restriction endonuclease (Fig. 4C). Damaged linear DNA containing DSBs was isolated by band purification and used in the end-joining assay.

Cell Extraction and Fractionation

HeLa S3 cells were grown as monolayers at 37°C in DMEM containing 10% (v/v) fetal bovine serum, 1% (v/v) nonessential amino acids, and 1% (v/v) penicillin/streptomycin (10,000 U/ml penicillin, 10,000 U/ml streptomycin sulfate). Nuclei were isolated from ~ 10 g (wet weight) freshly harvested, logarithmically growing cells by a modification of the method described previously (18). All cellular extraction procedures were performed at 4°C unless stated otherwise. Cells were harvested by scraping, then washed and pelleted twice in ice-cold PBS (800g). The cell pellet was resuspended in 2.5 volumes of hypotonic lysis buffer (10 mM Tris-HCl, pH 7.6, 1 mM DTT, 5 mM MgCl_2 , 1 mM EDTA, 10 mM pefablock, 10 $\mu\text{g/ml}$ aprotinin, 1.5 $\mu\text{g/ml}$ leupeptin, 100 $\mu\text{g/ml}$ bestatin, 1 $\mu\text{g/ml}$ pepstatin) and swollen on ice for 40 min. The cells were lysed by Dounce homogenization (40 strokes with the "loose" pestle). Lysis was estimated to be $\geq 90\%$ by Trypan Blue dye exclusion.

The homogenate was immediately brought to 250 mM sucrose, and nuclei were recovered by centrifugation at 1000g for 5 min. The nuclei were resuspended in an equal volume of hypotonic lysis buffer containing 250 mM sucrose and repelleted at 1000g for 10 min.

Isolated nuclei were resuspended in four volumes of nuclear extraction buffer [20 mM Tris-HCl, pH 7.6, 1 mM DTT, 2 mM EDTA, 20% (v/v) glycerol, 500 mM NaCl, 10 mM pefablock, 10 $\mu\text{g/ml}$ aprotinin, 1.5 $\mu\text{g/ml}$ leupeptin, 100 $\mu\text{g/ml}$ bestatin, 1 $\mu\text{g/ml}$ pepstatin]. After incubation on ice for 30 min with occasional gentle mixing, the extract was clarified by centrifugation at 25,000g for 20 min. The supernatant was dialyzed overnight against buffer A [20 mM Tris-HCl, pH 7.6, 1 mM DTT, 1 mM EDTA, 20% (v/v) glycerol, 25 mM NaCl, 0.2 mM PMSF].

Extracts were partially purified by chromatography on HiPrep Sephacryl 200, followed by DEAE Sephacel chromatography as described previously.

Immunodepletion

Immunoprecipitations were performed by mixing whole cell extract and anti-Ku80 (now known as XRRC5) antibody (BD Biosciences Pharmingen, San Diego, CA) at 4:1 (w/w) and incubating at 4°C for 1 h. Antibody-bound protein was removed from the extract with protein A sepharose and centrifugation. The immunodepleted supernatants were recovered and stored at -80°C until needed for enzyme assays.

End-Joining Assay

DNA DSB end-joining repair reactions were typically conducted in 50 μl total volume. Reactions contained 50 mM Tris-HCl (pH 8.2), 5 mM

MgCl₂, 1 mM ATP, 1 mM DTT, 5% polyethyleneglycol (PEG)-8000, 10 μg/ml aprotinin, 1.5 μg/ml leupeptin, 100 μg/ml bestatin, 10 mM pefablock, 100–125 ng substrate DNA, and partially purified HeLa nuclear extract, or commercial enzymes, as indicated in the figures. Repair reactions were stopped by the addition of 0.4% SDS and incubation at 65°C for 15 min. DNA was recovered by extraction with phenol:chloroform (1:1), and ethanol precipitation using 0.5 μg tRNA as a carrier. Repair products were identified by gel shift after 1% agarose electrophoresis and Vistra Green (VG) staining. Images were digitized with a FluorImager 595 system (Molecular Dynamics, Sunnyvale, CA) and quantified densitometrically using Gel-Pro software (Media Cybernetics, Silver Spring, MD).

Protein Assay

All protein determinations were made according to the method of Bradford (22) using bovine plasma gamma globulin as the standard.

RESULTS

In Vitro DSB Repair Assay

To assess the repair of DSBs of different complexities, we employed an *in vitro* DSB repair assay (18). In this assay, plasmid DNA is subjected to damage by an agent of choice and full-length linear DNA containing a single DSB is isolated by band purification and electroelution. This linear DNA substrate is then incubated with a partially purified human HeLa cell nuclear extract and repair products (dimers, trimers, etc.) are identified by gel shift. To make a direct detection approach practical and eliminate complex and time-consuming detection methods such as Southern blotting or radioactive methods, we employed the fluorescent DNA stain Vistra Green (VG). VG is capable of detecting <20 pg/band of double-stranded DNA (18, 23, 24). To establish that the NHEJ pathway is responsible for the end joining observed in our system, we examined the effect of immunodepleting XXRC5 on product formation. Western blot analysis of the immunodepleted HeLa extract demonstrated a slightly less than fivefold reduction in XXRC5 protein (Fig. 1A). Compared to the undepleted extract, the rate of product formation by the immunodepleted extract was reduced by an average of about fourfold (Fig. 1B). These results indicate a requirement for XXRC5 in the end-joining reaction and suggest that, under our assay conditions, NHEJ is the primary pathway responsible for product formation.

Currently, most *in vitro* DSB repair assays use DNA cut with restriction enzymes as the repair substrate. In many cases these substrates may be directly ligated or support combinations of polymerization and ligation that might not occur under normal circumstances (25–28). None of these methods make use of substrates that model naturally occurring DSB structures. As a result, these assays are focused upon measuring ligation. This is the final step of NHEJ; thus such assays do not permit the analysis of initiation involving end-group processing, as would be required at any naturally occurring “complex” or blocked DSB end (29) (Fig. 2).

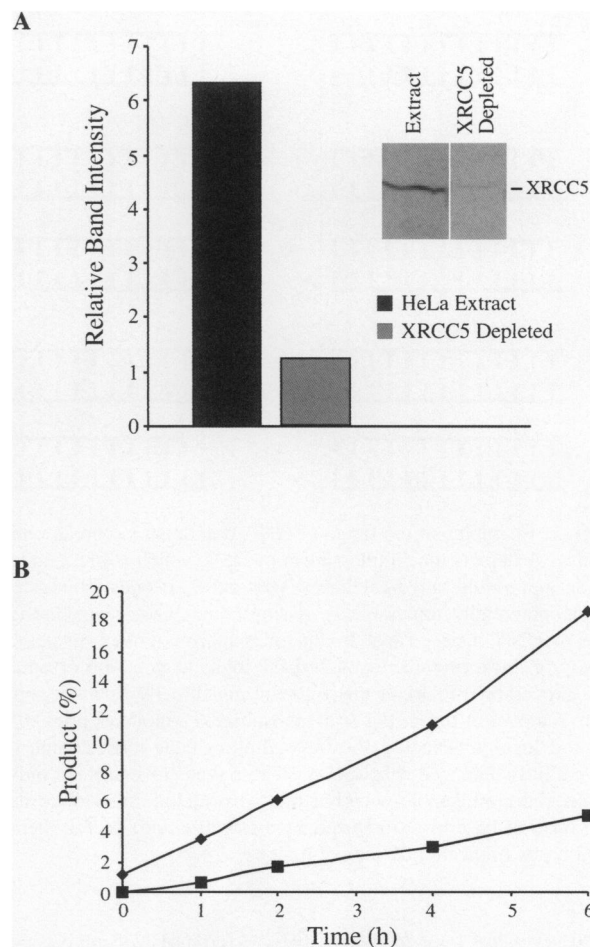


FIG. 1. HeLa extract XXRC5 immunodepletion. Panel A: The XXRC5 protein content of the extract was reduced fivefold after immunodepletion. Panel B: Kinetic analysis of repair after XXRC5 depletion. The depleted extract was employed in end-joining reactions with *Sma*I-linearized DNA as the substrate. End-joining activity was reduced proportionate to the reduction in XXRC5 protein content, yielding an average fourfold reduction in end joining. Untreated HeLa extract (◆), immunodepleted extract (■).

The radiomimetic drug bleomycin produces more complex unligatable double-strand breaks possessing 5'-P and 3'-phosphoglycolate (3'-PG) termini that are essentially blunt (30). Repair of these strand breaks requires removal and conversion of 3'-PG to 3'-OH groups.

Since 3'-PG represents approximately 50% of the termini at strand breaks produced by ionizing radiation (the remaining 50% contain 3'-P) (31), bleomycin-damaged DNA is frequently used as a model for radiation-induced DNA strand breaks during the study of repair or mutagenicity (19, 32–35). Yet there is considerable evidence that radiation-induced DSBs comprise a wide variety of structures ranging from fairly simple breaks containing only blocked ends to the more complex MDS (6, 36, 37).

DSBs can also be caused by ¹²⁵I, which is an Auger-electron emitter that decays by electron capture and internal conversion (38–40). Decay results in emission of about 20 low-energy electrons (below 1 keV) with ranges of several

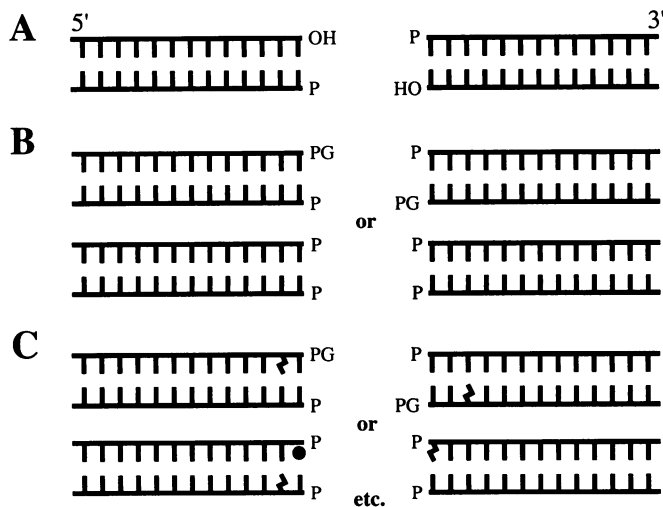


FIG. 2. Examples of the range of DNA double-strand break complexity. Panel A depicts the simplest form of DSB, which is blunt ended and contains opposable and ligatable 3'-OH and 5'-P ends. Breaks of this type are potentially repairable by a single enzymatic step, through the action of DNA ligase. Panel B illustrates more complex breaks similar to many of those produced by low-LET ionizing radiation or other oxidative processes. Breaks of this type are not directly ligatable, but they require removal of the 3'-PG or 3'-phosphate (P) moieties prior to alignment and ligation. Panel C shows examples of the most complex DSB type, multiply damaged sites (MDS). These types of DSBs not only contain blocked nonligatable ends but may also include nucleotide damage in the form of base loss (indicated by a closed circle) and/or chemically altered bases (indicated by jagged lines).

nanometers or less and a highly positively charged tellurium daughter atom. The simultaneous action of the low-energy Auger electrons, and possibly the charge neutralization of the daughter atom, are thought to produce the equivalent of a high-density energy deposition similar to that of high-LET radiations like α particles at the decay site (41–43). Decay of ^{125}I incorporated into one strand of a DNA duplex (as iododeoxyuridine or labeled aminoacridines) produces strand breaks located within about 10 bp of the decay site with an efficiency approaching one DSB/decay (40, 44, 45). We used a ^{125}I -labeled TFO to induce DSBs in a target duplex DNA molecule at an efficiency of nearly one DSB/decay (46).

We employed substrates created by each of these methods to produce linear DNA containing increasingly complex DSB structures. By incorporating these substrates into individual repair reactions, we were able to assess their impact upon the NHEJ pathway.

DSB Induction by Bleomycin

Since bleomycin produces several single-strand breaks (SSBs) for every DSB, damaged DNA contains a dose-dependent mixture of topological forms (supercoiled, open circular, and linear). In contrast to restriction enzyme treatment, the incremental production of DSBs by bleomycin restricts the amount of linear DNA that can be produced from a given weight of plasmid. Consequently, the yield of

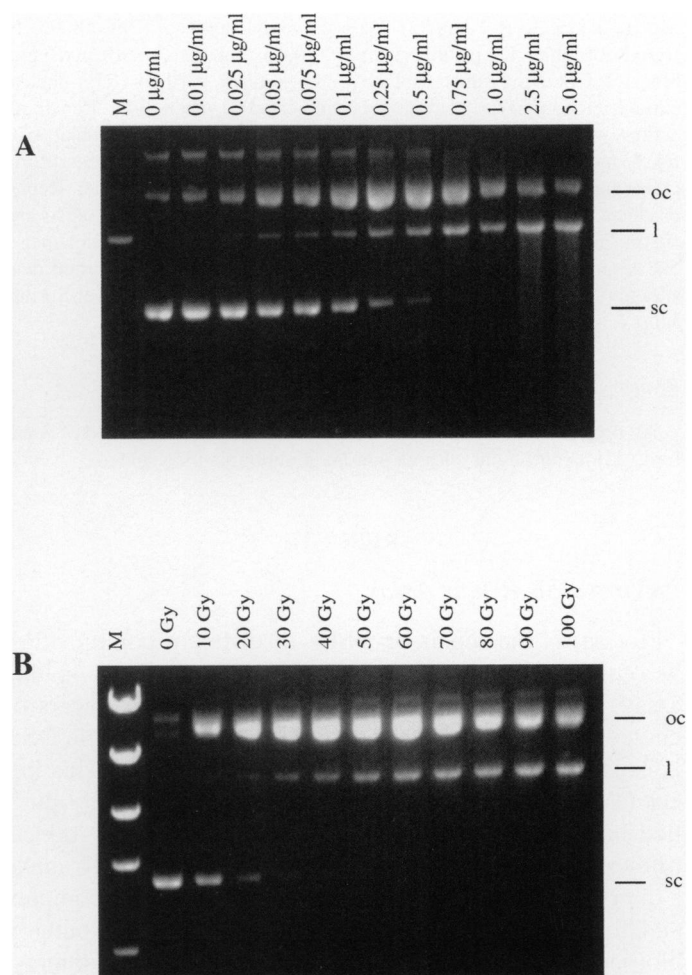


FIG. 3. Panel A: Bleomycin damage dose response. Concentrations are reported as μg bleomycin/ml of DNA solution treated ($150 \mu\text{g}$ DNA/ml). Lane M contains *EcoRI*-linearized pSP189 as a marker. The positions of the open-circular (oc), linear (l) and supercoiled (sc) forms of pSP189 DNA are indicated to the right of the gel. Panel B: ^{60}Co γ -ray DNA damage dose response. Lane M contains high mass markers (Invitrogen). Plasmid DNA was irradiated in 50 mM sodium phosphate, pH 7.2, at the doses indicated. In both panels A and B, open circular DNA (containing single-strand breaks) and linear DNA (containing a single double-strand break) are produced in a dose-dependent manner, with a concomitant loss of supercoiled DNA.

linear DNA is low in comparison to restriction enzyme digestion. To maximize the yield of linear plasmid containing bleomycin-induced DSBs, a bleomycin dose-response experiment was conducted (Fig. 3A). Plasmid damaged by $0.5 \mu\text{g}$ bleomycin/ml ($3.4 \times 10^{-3} \mu\text{g}$ bleomycin/ μg DNA) was found to produce the greatest yield of linear DNA while retaining the highest efficiency of repair activity (18).

DSB Induction by ^{60}Co γ Rays

Figure 3B shows a ^{60}Co γ -ray DNA damage dose response. Plasmid DNA (pSP189) was irradiated as indicated producing open circular DNA, and linear DNA containing a single double-strand break, in a dose-dependent manner with a concomitant loss of supercoiled DNA. The 30-Gy

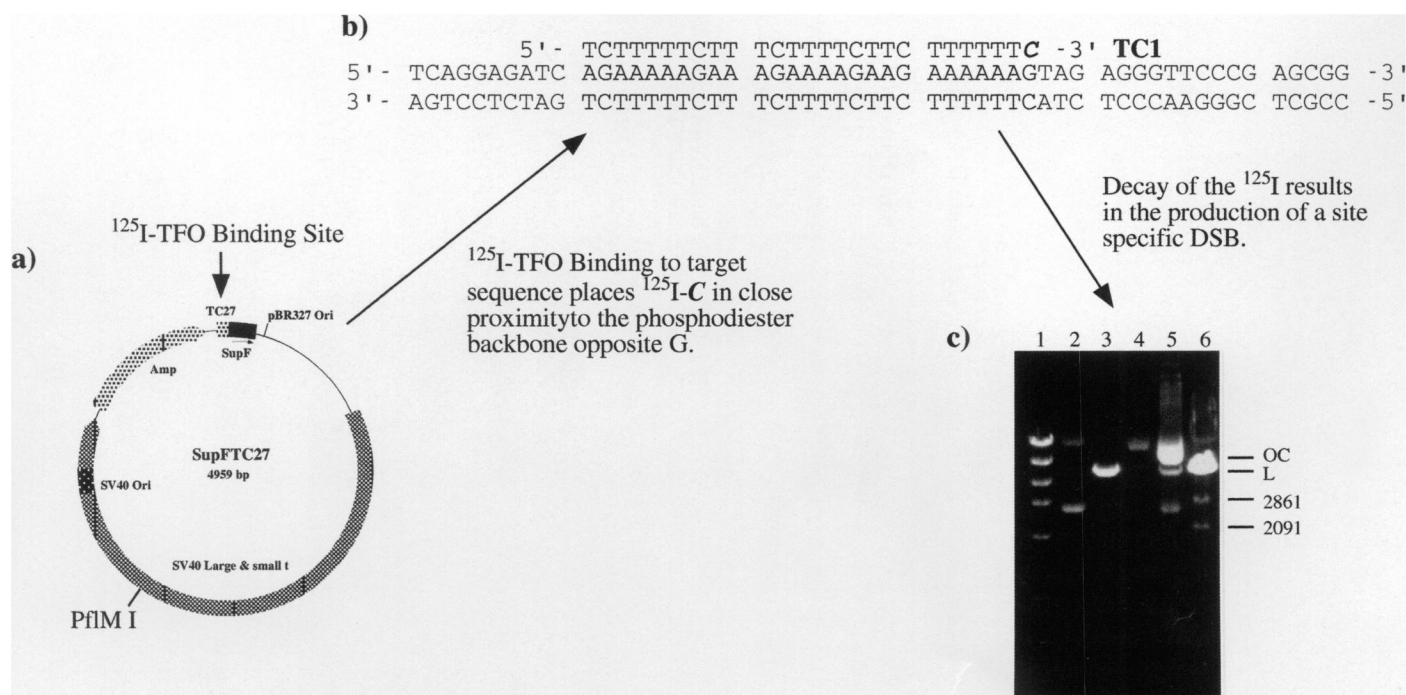


FIG. 4. Production of site-specific ^{125}I induced DSB. Site specific positioning of the ^{125}I is accomplished using a TFO delivery vehicle. Production of site-specific DSBs in the target sequence of plasmid TC27 (panels a and b) is demonstrated by the formation of appropriate-sized fragments (2861 bp and 2091 bp) after cleavage of the damaged plasmid with restriction enzyme *PflMI*. Panel c: lane 1, high mass markers; lane 2, pTC27 supercoiled DNA marker; lane 3, pTC27 linear DNA marker; lane 4, pTC27 open circular DNA marker; lane 5, 0.5 μg damaged plasmid; lane 6, 0.5 μg *PflMI*-cut damaged plasmid.

dose produced a proportional yield of DNA forms closest to that of the 0.5- $\mu\text{g}/\text{ml}$ bleomycin reactions. Therefore, linear DNA isolated from the 30-Gy irradiation mixture was employed as a substrate in end-joining assays.

Site-Specific DSB Induction by ^{125}I

Using the model system shown in Fig. 4, the ^{125}I -labeled TFO, TC1, was used to produce a bona fide site-specific radiation-induced DNA DSB. The polypyrimidine 27 mer TC1 TFO was designed to recognize and bind in an anti-parallel orientation to positions 7–33 of pTC27, placing the 3'-end of the TFO immediately 5' to the plasmid *SupF* gene (Fig. 4A and B). The triple helical structure places the [5- ^{125}I]dCMP residue at position 27 of the TFO close to the phosphodiester backbone of pTC27 opposite the G at position 33. The resulting ^{125}I -C•GC triplet produces localized DSBs that typically range from 5 bases upstream to 5 bases downstream of the ^{125}I -C position (21, 46, 47). The damaged DNA product was distributed in three forms: supercoiled DNA, open circular DNA and linear DNA (Fig. 4C, lane 5). To demonstrate site-specific DSB production in pTC27, an amount of damaged DNA equivalent to that run in lane 5 was cleaved with restriction enzyme *PflMI*. The unique *PflMI* restriction site is nearly opposite the TFO-binding site (Fig. 4A). Therefore, *PflMI* cleavage of plasmid molecules that have accumulated site-specific DSBs results in the production of two DNA fragments of 2861 bp and 2091 bp, respectively. In contrast, plasmids that con-

tain SSBs, or are otherwise intact, will linearize and run as linear DNA after electrophoresis. Production of two appropriate-size fragments after cleavage of the damaged plasmid DNA demonstrates TFO-mediated site-specific DSB induction (Fig. 4C, lane 6). Linear DNA containing site-specific DSBs was isolated to serve as a substrate in the repair assay.

Rejoining of DSBs by Recombinant and Human Enzymes

To examine the structure of DSBs produced by different agents and compare their capacity to support end joining, we employed recombinant bacterial enzymes (*E. coli* endonuclease IV; phage T4 DNA ligase) and human HeLa enzymes. Endonuclease IV (endo IV) is a class II AP endonuclease that is capable of cleaving 3'-nucleotide fragments at DNA strand breaks to produce a 3'-OH that can serve as a substrate for ligation and polymerization (48). T4 DNA ligase rejoins strand breaks possessing 3'-OH and 5'-P ends, and it is highly efficient at blunt end ligation in addition to ligation of complementary overhangs. It has also been reported to have a limited ability to join overhangs containing a single-base mismatch and to join short overhangs to blunt ends (49). DNA linearized by ^{125}I , γ rays, bleomycin or *StuI* was treated with *E. coli* endo IV and T4 DNA ligase either alone or in combination (Figs. 5 and 6). Endo IV treatment alone had no effect on the migration of linearized substrates (Fig. 5A, lanes 3 and 8; Fig. 6A and C, lane 3). In contrast, T4 ligase produced rejoining

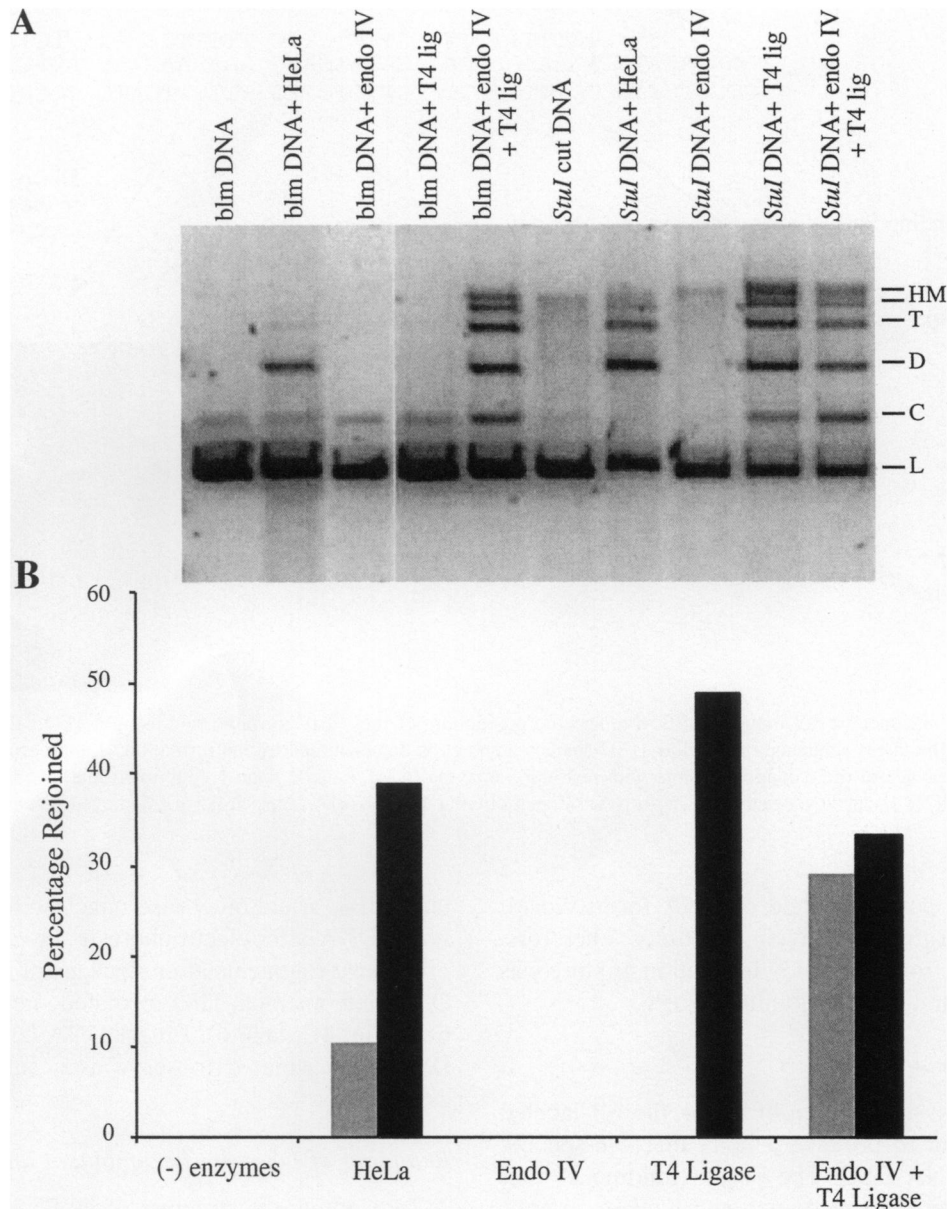


FIG. 5. Differential repair of bleomycin-induced DSB ends and *StuI*-induced blunt ends in the presence of HeLa cell extract or recombinant bacterial enzymes. Standard, repair reactions were performed with DNA linearized by either 0.5 μg bleomycin/ml or *StuI* digestion. The repair reactions contained either, 15 μg HeLa extract, 2 U *E. coli* endonuclease IV, 5 U T4 DNA ligase, or combinations as indicated. Reactions were incubated at 17°C for 18 h. Panel A: Reaction products visualized in a 1% agarose gel with Vistra Green. The positions of the DNA substrate and products are indicated to the right of the gel as linear (L), circular (C), dimer (D), trimer (T), and high-molecular-weight multimers (HM). Panel B: The data from the gels were plotted as the percentage of linear substrate DNA converted to end-joined product. Reactions performed with bleomycin-linearized DNA substrates are represented by gray bars while those performed with the *StuI*-linearized DNA are represented by the black bars. This figure is reproduced with permission from Pastwa *et al.* (18).

products in the presence of *StuI*-cut DNA but not with the more complex substrates (Fig. 5A, lane 9; Fig. 6A and C, lane 4). However, when these substrates were reacted with endo IV and T4 DNA ligase in combination, repair products are formed with almost identical distribution in DNA linearized with *StuI*, bleomycin, γ rays or ^{125}I (Fig. 5A, lanes 5 and 10; Fig. 6A and C, lane 5). The bleomycin-linearized substrate results not only confirmed its DSB ends to be blocked (Fig. 5A, lanes 4 and 5) but, due to the efficient end joining obtained with the endo IV/T4 DNA

ligase combination, also supported previous reports of the largely blunt-ended structure of bleomycin-induced DSBs (18, 30). The yield of end-joined product for bleomycin- and *StuI*-cut DNA in the presence of recombinant enzymes was essentially the same (30–35%) (Fig. 5B). This demonstrates that only the 3'-PG nucleotide remnants at the bleomycin-induced DSBs affect the ability of these substrates to support end joining. Therefore, collateral SSB damage introduced into the DNA by bleomycin, or potential damage resulting from handling during purification,

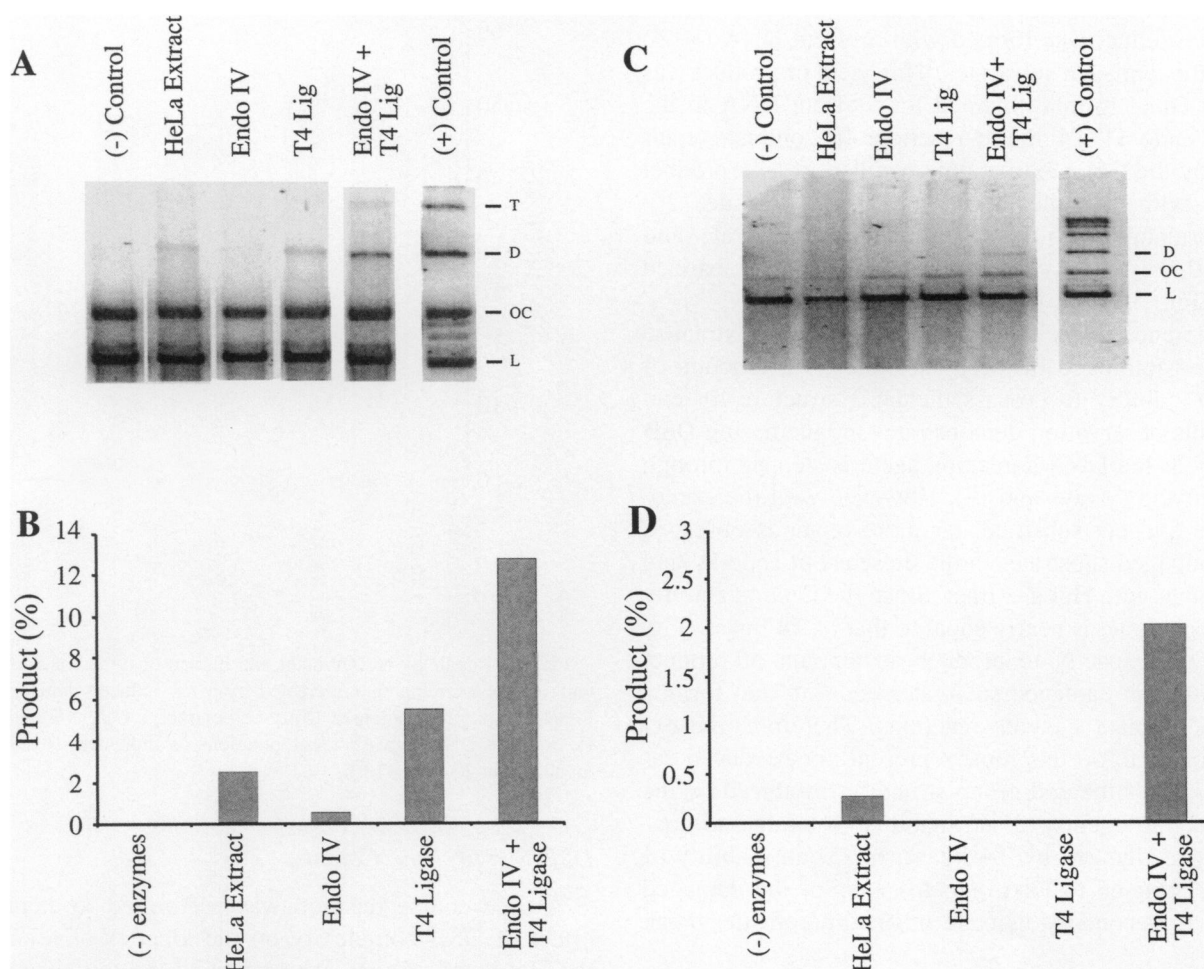


FIG. 6. Repair of 30 Gy γ -ray-induced or site-specific 125 I-TFO-induced DSBs by recombinant and human enzymes. Reaction mixtures contained 15 μ g cell extract, 2 U *E. coli* endonuclease IV, 5 U T4 DNA ligase, or combinations as indicated. Reactions were incubated at 17°C for 18 h. Panel A: Reaction products of the γ -ray-linearized DSB repair substrate visualized in a 1% agarose gel with Vistra Green. The position of the DNA substrate and products are indicated to the right of the gel as linear (L), circular (C), dimer (D), and trimer (T). Panel B: The data from the gel were plotted as the percentage of linear substrate DNA converted to end-joined product. Panel C: Reaction products of the 125 I-TFO-linearized DSB repair substrate visualized in a 1% agarose gel with Vistra Green. Panel D: The data from the gel were plotted as the percentage of linear substrate DNA converted to end-joined product.

does not significantly reduce the capacity of the substrate to support end joining with respect to blunt DSB ends of otherwise undamaged *StuI*-cut DNA.

In contrast, DSBs produced by γ rays and 125 I are progressively more refractory to direct end joining by the combined action of endo IV and T4 ligase, supporting the assumption that these molecules possess more complex or heterogeneous end structures. The γ -ray-linearized substrate supported less than half (12%) of the endo IV/T4 ligase-mediated end joining observed for the bleomycin- or *StuI*-linearized substrates. Surprisingly, in the presence of T4 ligase alone, the γ -ray-linearized DNA also supported a substantial amount of end joining (5%), suggesting that up to 40% of the γ -ray-linearized molecules capable of supporting direct end joining possess 3'-OH ends and do not require processing prior to ligation.

In contrast, reaction of the 125 I-linearized substrate with T4 ligase alone did not result in any product formation,

whereas 2% of the substrate was converted to product by the combined action of endo IV and T4 ligase (Fig. 6B and D). These results also show some important structural characteristics of the 125 I-induced DSBs. The observation that up to 2% of the 125 I induced DSBs can be rejoined by the combined action of T4 DNA ligase and endo IV demonstrates that at least a subpopulation of these breaks must contain 3'-nucleotide fragments that are recognizable by endo IV. Also, the lack of rejoining with the remaining 98% of the 125 I-induced DSBs indicates that these breaks consist of a more complex structure than the 2% of ends that were capable of supporting rejoining. This suggests a possible heterogeneity of DSB end conformations that are largely unligatable and/or the presence of end-group structures incapable of being recognized by endo IV.

The linear substrate DNAs were also incubated for repair by HeLa cell extract. Although high-molecular-weight repair products were formed with all four substrates, substan-

tially more product was formed with *StuI*-cut DNA (40%) than with the damaged substrates. This yield of product was essentially equal to that obtained for *StuI*-cut DNA in the combined endo IV/T4 ligase reaction. In contrast, repair mediated by the HeLa extract only resulted in 10% product formation with the bleomycin-linearized substrate, 2% product formation with the γ -ray-linearized substrate, and less than 0.5% product formation with the ^{125}I -linearized substrate (Fig. 5B, and Fig. 6B and D).

The difference in the ability of the HeLa cell extract to catalyze end joining with these substrates is a function of the extract's ability to process the DSB structure for end joining. This observation demonstrates the increasing DSB complexity as the DNA-damaging agent is stepped through *StuI*, bleomycin, γ rays and ^{125}I . However, with the exception of the *StuI*-cut substrate, far more repair is observed with the damaged substrates in the presence of endo IV and T4 ligase than with HeLa extract. Since the ligation activity of the HeLa extract is nearly equal to that of T4 ligase (Fig. 5), it has the capacity to produce an amount of product from each of the damaged substrates equal to that formed in the recombinant enzyme reactions. Therefore, the extract's inability to do this must represent (1) a reduced capacity to process the end-group structures produced by the DNA-damaging agents, (2) an inability to ligate end conformations recognized by T4 ligase, or (3) an inability of the NHEJ complex to load onto the ends of the damaged DNA due to secondary damage upstream from the break ends.

To test the potential of secondary damage upstream of the break ends to affect repair by the NHEJ pathway, but not direct end joining mediated by T4 ligase, γ -ray-damaged open circular DNA was isolated and cut to completion with *StuI* (data not shown). The *StuI*-linearized γ -ray-damaged open circular DNA was employed in a series of reactions similar to those described above (Fig. 7). This substrate supported direct end joining by T4 ligase at an efficiency equal to that observed with otherwise undamaged DNA cut with *StuI*. This demonstrates that although the DNA contains γ -ray-induced SSBs and base damage, this secondary damage does not affect the ability of the restriction enzyme-induced DSBs to be ligated. Although the *StuI*-linearized γ -ray-damaged open circular DNA was readily ligatable, HeLa extract-mediated end joining of this substrate was only 2%. This equals the amount of end joining the HeLa extract produced with the γ -ray-linearized substrate (Fig. 6B). These results suggest that although the HeLa extract had a capacity to rejoin the *StuI*-cut ends of the γ -ray-damaged open circular DNA that was equal to that of T4 ligase, secondary damage upstream of the DSB inhibits interaction with the NHEJ complex, subsequent end alignment, and ligation. Furthermore, HeLa extract-mediated end joining of the γ -ray-linearized DNA (Fig. 6) may be influenced by lesions proximal to the DSB end as well as by processing of DSB end-group blocking structures.

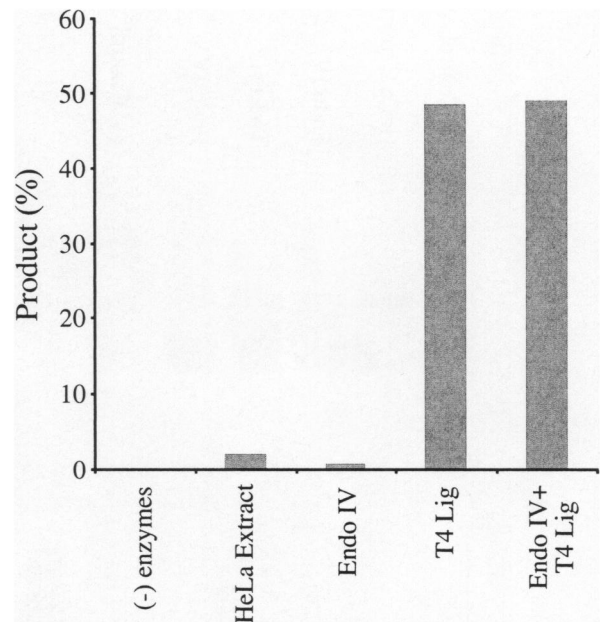


FIG. 7. Repair by recombinant and human enzymes of *StuI*-cut blunt ends in open circular DNA created by γ -ray-induced damage (30 Gy). Reaction mixtures contained 15 μg cell extract, 2 U *E. coli* endonuclease IV, 5 U T4 DNA ligase, or combinations as indicated. Reactions were incubated at 17°C for 18 h.

DSB Repair Time Course

A time course reaction was performed to examine the effect of DSB complexity on the kinetics of rejoining by the HeLa cell extract. We compared the initial rate of end joining on *StuI*-, bleomycin-, γ -ray- and ^{125}I -linearized substrates. These assays indicate a sixfold lower rate of repair for bleomycin-induced DSBs than for the ligatable blunt-ended DSBs produced by *StuI* (Fig. 8). Repair of bleomycin-induced DSBs appears to involve a lag phase between 0 and 1 h that is not evident in the end-joining reactions with blunt-ended DNA. Repair of γ -ray-induced DSBs occurred at a 15-fold lower rate than repair of *StuI*-induced DSBs. Repair of the ^{125}I -TFO-induced DSBs was nearly undetectable, and it proceeded at a rate at least twofold lower than that observed for γ -ray-induced DSBs.

DISCUSSION

In the present work, we examined the ability of the human NHEJ pathway to directly rejoin DSBs with a range of lesion complexities and structural organization that exist in naturally occurring DSBs similar to those expected *in vivo*. We established that end joining by HeLa extracts, as measured in our assay, is directly dependent upon the presence of XXRC5 (Fig. 1), thus implicating the KU protein-driven NHEJ pathway as the mechanism of repair mediated by the extract. This finding is further supported by the lack of closed-circular product formation by the HeLa extract (Fig. 5A). Production of closed circles has been shown to be characteristic of *in vitro* reactions mediated by direct

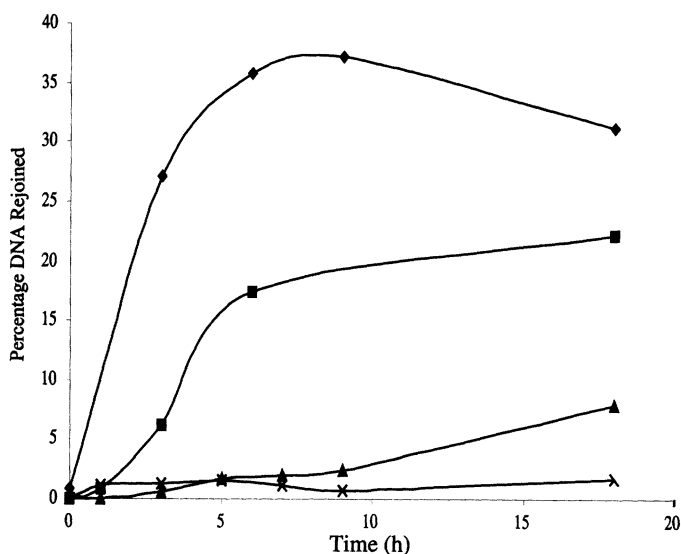


FIG. 8. Time course of the reactions for HeLa cell extract-mediated repair of DNA containing *StuI*-induced blunt end DSBs (closed diamonds), bleomycin-induced DSBs (closed squares), γ -ray-induced DSBs (closed triangles), and site-specific ^{125}I -induced DSBs (crosses). Reactions were conducted at 17°C with $15\ \mu\text{g}$ of HeLa extract for the times indicated.

DNA ligase IV/XRCC4 end joining but not by the complete KU/PRKDC1/DNA ligase IV/XRCC4 NHEJ complex (50).

Our findings indicate that as the structural complexity of a DSB lesion increases, the ability of the NHEJ pathway to rejoin the break decreases. This direct observation of DSB end joining further supports the theory put forward by numerous observations that the increasing lethality of ionizing radiation observed with increasing radiation LET is a function of increasing DSB complexity. The more structurally complex the break, the more difficult it is to process for repair. Comparative analysis for repair of DSBs produced by different agents demonstrates damage-dependent differences not only in the repair reaction but also in the structural complexity of the lesion being repaired. When HeLa cell extract was the source of repair activity, ^{125}I -, γ -ray- and bleomycin-induced DSBs were rejoined much less effectively than readily ligatable, *StuI*-induced DSBs (Figs. 5 and 6). In the HeLa extract NHEJ reactions, this may be largely a function of increased SSBs and/or base damage proximal to the DSB end as depicted in Fig. 2C. Bleomycin and, to a larger extent, γ -ray- and ^{125}I -induced DSBs are accompanied by secondary lesions proximal to the DSB end. These secondary lesions appear to inhibit repair by the NHEJ complex even at readily ligatable DSBs ends. This is demonstrated by the inability of the HeLa cell extract to promote efficient ligation of *StuI* restriction enzyme DSBs produced by cutting open circular DNA created by γ -ray damage. *StuI* efficiently and completely linearized the γ -ray-damaged open circular DNA; moreover, the *StuI*-induced DSBs were efficiently ligated by T4 DNA ligase, demonstrating that the γ -ray-induced secondary damage did not interfere with the enzyme's ability to interact with

the DSB ends (Fig. 7). Therefore, secondary lesions proximal to the DSB end, which most likely occur within or near the footprint of the eukaryotic NHEJ complex (KU/PRKDC/DNA ligase IV/XRCC4), are highly inhibitory to the NHEJ reaction. This result is consistent with the nature of the DNA-damaging mechanisms of the DNA-damaging agents tested in this study and with the relative likelihood of secondary lesions being produced close to the DSB end. In the case of bleomycin, approximately six SSBs are produced for every DSB, resulting in an average frequency of one SSB for every 827 bp of our target plasmid DNA (51, 52). Therefore, based upon a footprint of approximately 25 bp per KU heterodimer, about 3% of the bleomycin-linearized molecules in our reaction would be likely to contain an SSB that might interfere with loading of the NHEJ complex (53). In the case of γ -ray-induced damage, estimates of up to 60% of DSBs consisting of a complex structure including proximal base damage have been reported, while as many as 90% of the DSBs induced by high-LET radiation are estimated to consist of these complex structures (54). Because of the highly localized energy deposition of ^{125}I , ^{125}I -induced DSBs may approach 100% for complexity proximal to the DSB end (55).

Our observation of a reduced repair reaction rate for DSBs blocked by 3'-PG compared to 3'-OH ends is consistent with the observations of others (56, 57). The apparent time lag in initiating repair for bleomycin-induced DSBs compared to *StuI*-induced DSBs may reflect the need to remove 3'-PG from the substrate prior to formation of multimeric products; The progressive reduction in product formation in the reactions employing γ -ray- and ^{125}I -induced DSBs indicates the increasing structural complexity of these lesions.

By employing the bacterial enzymes, endonuclease IV and T4 DNA ligase, we have demonstrated for the first time the DSBs produced by ^{125}I to be blocked by 3'-nucleotide fragments (Fig. 6C). The 5'-end group chemistry of Auger-electron-induced DSBs have been determined indirectly by Maxam-Gilbert sequencing on target sequences that had been damaged by bound ^{125}I -labeled TFOs (21, 46). These reactions were performed with 3'-end labeled duplexes, and they indicated that the 5'-end groups of the break sites are 5'-P. No determination of the 3'-end structure has been reported. Identification of a complex 3'-end structure at ^{125}I -induced DSBs, in addition to the highly inhibitory effect of damage proximal to the DSB ends, may begin to explain the poor repair observed by us ($\geq 2\%$, Fig. 6D and Fig. 8) and many others, for Auger-electron-induced DSBs (42, 55, 58–60). Our results also indicate that the majority of ^{125}I -induced DSBs are not directly ligatable after 3'-end processing by endo IV. In contrast, at least a small subset of Auger-electron-induced DSBs are ligatable after 3'-end processing, indicating that the 5'-ends possess PO_4 groups. Furthermore, based upon the range of T4 DNA ligase structural recognition, these results also indicate that the possible range of DSB end conformations consists of directly op-

posable blunt ends, complementary or single-base mismatched overhangs of equal length, or short overhangs ligated to blunt ends. These results, in conjunction with the comparatively poor yield of rejoined products observed in the time-course reactions, suggest that DSBs produced by ^{125}I are much more structurally complex than those produced by γ rays and by bleomycin.

The differential repair results obtained with direct ligation reactions using prokaryotic enzymes and end-joining reactions catalyzed by NHEJ, and in particular the results observed for inhibition of NHEJ by damage proximal to the DSBs site, indicate the need to construct substrates in which the DSB end-group structure and damage proximal to the DSB end can be investigated independently. This will allow a detailed analysis of the contribution of each lesion type and the mechanism(s) by which each lesion affects the ability of complex DSB lesions to be repaired.

Received: September 17, 2001; accepted: September 11, 2002

REFERENCES

1. L. F. Povirk, DNA damage and mutagenesis by radiomimetic DNA-cleaving agents: Bleomycin, neocarzinostatin and other enediynes. *Mutat. Res.* **355**, 71–89 (1996).
2. J. Dahm-Daphi, C. Sass and W. Alberti, Comparison of biological effects of DNA damage induced by ionizing radiation and hydrogen peroxide in CHO cells. *Int. J. Radiat. Biol.* **76**, 67–75 (2000).
3. M. A. Chaudhry and M. Weinfeld, Reactivity of human apurinic/aprimidinic endonuclease and *Escherichia coli* exonuclease III with bistranded abasic sites in DNA. *J. Biol. Chem.* **272**, 15650–15655 (1997).
4. B. N. Ames, Micronutrient deficiencies—A major cause of DNA damage. In *Cancer Prevention: Novel Nutrient and Pharmaceutical Developments* (H. L. Bradlow, J. Fishman and M. P. Osborne, Eds.), pp. 87–106. New York Academy of Sciences, New York, 1999.
5. P. Pfeiffer, The mutagenic potential of DNA double-strand break repair. *Toxicol. Lett.* **96–97**, 119–129 (1998).
6. P. Pfeiffer, W. Goedecke and G. Obe, Mechanisms of DNA double-strand break repair and their potential to induce chromosomal aberrations. *Mutagenesis* **15**, 289–302 (2000).
7. P. A. Jeggo, Identification of genes involved in repair of DNA double-strand breaks in mammalian cells. *Radiat. Res.* **150** (Suppl.), S80–S91 (1998).
8. C. R. Bertocini and R. Meneghini, DNA strand breaks produced by oxidative stress in mammalian cells exhibit 3'-phosphoglycolate termini. *Nucleic Acids Res.* **23**, 2995–3002 (1995).
9. G. W. Buchko, and M. Weinfeld, Influence of nitrogen, oxygen, and nitroimidazole radiosensitizers on DNA damage induced by ionizing radiation. *Biochemistry* **32**, 2186–2193 (1993).
10. W. D. Henner, S. M. Grunberg and W. A. Haseltine, Enzyme action at 3' termini of ionizing radiation-induced DNA strand breaks. *J. Biol. Chem.* **258**, 15198–15205 (1983).
11. J. F. Ward, Complexity of damage produced by ionizing radiation. *Cold Spring Harbor Symp. Quant. Biol.* **65**, 377–382 (2000).
12. J. R. Milligan, J. A. Aguilar, R. A. Paglinawan, J. F. Ward and C. L. Limoli, DNA strand break yields after post-high LET irradiation incubation with endonuclease-III and evidence for hydroxyl radical clustering. *Int. J. Radiat. Biol.* **77**, 155–164 (2001).
13. J. O. Blaisdell and S. S. Wallace, Abortive base-excision repair of radiation-induced clustered DNA lesions in *Escherichia coli*. *Proc. Natl. Acad. Sci. USA* **98**, 7426–7430 (2001).
14. S. S. Wallace, Enzymatic processing of radiation-induced free radical damage in DNA. *Radiat. Res.* **150** (Suppl.), S60–S79 (1998).
15. L. Harrison, Z. Hatahet and S. S. Wallace, *In vitro* repair of synthetic ionizing radiation-induced multiply damaged DNA sites. *J. Mol. Biol.* **290**, 667–684 (1999).
16. J. L. Ravanat, P. Di Mascio, G. R. Martinez, M. H. G. Medeiros and J. Cadet, Singlet oxygen induces oxidation of cellular DNA. *J. Biol. Chem.* **275**, 40601–40604 (2000).
17. E. Hoglund and B. Stenerlow, Induction and rejoining of DNA double-strand breaks in normal human skin fibroblasts after exposure to radiation of different linear energy transfer: Possible roles of track structure and chromatin organization. *Radiat. Res.* **155**, 818–825 (2001).
18. E. Pastwa, R. D. Neumann and T. A. Winters, *In vitro* repair of complex unligatable oxidatively induced DNA double-strand breaks by human cell extracts. *Nucleic Acids Res.* **29**, e78 (2001).
19. T. A. Winters, M. Weinfeld and T. J. Jorgensen, Human HeLa-cell enzymes that remove phosphoglycolate 3'-end groups from DNA. *Nucleic Acids Res.* **20**, 2573–2580 (1992).
20. K. Mezhevaya, T. A. Winters and R. D. Neumann, Gene targeted DNA double-strand break induction by I-125-labeled triplex-forming oligonucleotides is highly mutagenic following repair in human cells. *Nucleic Acids Res.* **27**, 4282–4290 (1999).
21. I. G. Panyutin and R. D. Neumann, Sequence-specific DNA breaks produced by triplex-directed decay of iodine-125. *Acta Oncol.* **35**, 817–23 (1996).
22. M. M. Bradford, A rapid and sensitive method for the quantitation of microgram quantities of protein utilizing the principle of protein-dye binding. *Anal. Biochem.* **72**, 248–254 (1976).
23. S. D. O'Dell, X. H. Chen and I. N. M. Day, Higher resolution microplate array diagonal gel electrophoresis: Application to a multiallelic minisatellite. *Hum. Mutat.* **15**, 565–576 (2000).
24. R. S. Madabhushi, M. Vainer, V. Dolnik, S. Enad, D. L. Barker, D. W. Harris and E. S. Mansfield, Versatile low-viscosity sieving matrices for non-denaturing DNA separations using capillary array electrophoresis. *Electrophoresis* **18**, 104–111 (1997).
25. P. North, A. Ganesh and J. Thacker, The rejoining of double-strand breaks in DNA by human cell extracts. *Nucleic Acids Res.* **18**, 6205–6210 (1990).
26. R. M. Mason, J. Thacker and M. P. Fairman, The joining of non-complementary DNA double-strand breaks by mammalian extracts. *Nucleic Acids Res.* **24**, 4946–4953 (1996).
27. P. Baumann and S. C. West, DNA end-joining catalyzed by human cell-free extracts. *Proc. Natl. Acad. Sci. USA* **95**, 14066–14070 (1998).
28. E. Feldmann, V. Schmiemann, W. Goedecke, S. Reichenberger and P. Pfeiffer, DNA double-strand break repair in cell-free extracts from Ku80-deficient cells: Implications for Ku serving as an alignment factor in non-homologous DNA end joining. *Nucleic Acids Res.* **28**, 2585–2596 (2000).
29. J. Thacker, The study of responses to 'model' DNA breaks induced by restriction endonucleases in cells and cell-free systems: Achievements and difficulties. *Int. J. Radiat. Biol.* **66**, 591–596 (1994).
30. L. F. Povirk, Y. H. Han and R. J. Steighner, Structure of bleomycin-induced DNA double-strand breaks: Predominance of blunt ends and single-base 5' extensions. *Biochemistry* **28**, 5808–5814 (1989).
31. W. D. Henner, L. O. Rodriguez, S. M. Hecht and W. A. Haseltine, Gamma-ray induced deoxyribonucleic acid strand breaks. *J. Biol. Chem.* **258**, 711–713 (1983).
32. M. E. Dar and T. J. Jorgensen, Deletions at short direct repeats and base substitutions are characteristic mutations for bleomycin-induced double- and single-strand breaks, respectively, in a human shuttle vector system. *Nucleic Acids Res.* **23**, 3224–3230 (1995).
33. M. E. Dar, T. A. Winters and T. J. Jorgensen, Identification of defective illegitimate recombinational repair of oxidatively-induced DNA double-strand breaks in ataxia-telangiectasia cells. *Mutat. Res.* **384**, 169–179 (1997).
34. T. A. Winters, W. D. Henner, P. S. Russell, A. McCullough and T. J.

- Jorgensen, Removal of 3'-phosphoglycolate from DNA strand-break damage in an oligonucleotide substrate by recombinant human apurinic/apyrimidinic endonuclease I. *Nucleic Acids Res.* **22**, 1866–1873 (1994).
35. P. Wang, R. H. Zhou, Y. Zou, C. K. Jackson-Cook and L. F. Povirk, Highly conservative reciprocal translocations formed by apparent joining of exchanged DNA double-strand break ends. *Proc. Natl. Acad. Sci. USA* **94**, 12018–12023 (1997).
 36. J. F. Ward, DNA damage produced by ionizing radiation in mammalian cells—identities, mechanisms of formation, and reparability. *Prog. Nuc. Acid Res. Mol. Biol.* **35**, 95–125 (1988).
 37. J. F. Ward, The yield of DNA double-strand breaks produced intracellularly by ionizing-radiation—a review. *Int. J. Radiat. Biol.* **57**, 1141–1150 (1990).
 38. L. E. Feinendegen, Biological damage from the Auger effect, possible benefits. *Radiat. Environ. Biophys.* **12**, 85–99 (1975).
 39. L. E. Feinendegen, P. Henneberg and G. Tisljar-Lentulis, DNA strand breakage and repair in human kidney cells after exposure to incorporated iodine-125 and cobalt-60 γ -rays. *Cur. Top. Radiat. Res. Q.* **12**, 436–452 (1977).
 40. R. F. Martin and W. A. Haseltine, Range of radiochemical damage to DNA with decay of iodine-125. *Science* **213**, 896–898 (1981).
 41. R. W. Howell, Radiation spectra for Auger-electron emitting radionuclides: report No. 2 of AAPM Nuclear Medicine Task Group No. 6. *Med. Phys.* **19**, 1371–1383 (1992).
 42. K. S. R. Sastry, Biological effects of the Auger emitter I-125—a review—report No. 1 of AAPM Nuclear Medicine Task Group No. 6. *Med. Phys.* **19**, 1361–1370 (1992).
 43. I. G. Panyutin, T. A. Winters, L. E. Feinendegen and R. D. Neumann, Development of DNA-based radiopharmaceuticals carrying Auger-electron emitters for anti-gene radiotherapy. *Q. J. Nucl. Med.* **44**, 256–267 (2000).
 44. R. E. Krisch, F. Krasin and C. J. Sauri, DNA breakage, repair and lethality after ^{125}I decay in *rec+* and *recA* strains of *Escherichia coli*. *Int. J. Radiat. Biol.* **29**, 37–50 (1976).
 45. D. E. Charlton, H. Nikjoo and J. L. Humm, Calculation of initial yields of single-strand and double-strand breaks in cell-nuclei from electrons, protons and alpha-particles. *Int. J. Radiat. Biol.* **56**, 1–19 (1989).
 46. I. G. Panyutin and R. D. Neumann, Sequence-specific DNA double-strand breaks induced by triplex forming ^{125}I labeled oligonucleotides. *Nucleic Acids Res.* **22**, 4979–4982 (1994).
 47. I. G. Panyutin and R. D. Neumann, Radioprobng of DNA: Distribution of DNA breaks produced by decay of ^{125}I incorporated into a triplex-forming oligonucleotide correlates with geometry of the triplex. *Nucleic Acids Res.* **25**, 883–887 (1997).
 48. M. Weinfeld, J. Lee, R. Q. Gu, F. Karimi-Busheri, D. Chen and J. Allalunis-Turner, Use of a postlabelling assay to examine the removal of radiation-induced DNA lesions by purified enzymes and human cell extracts. *Mutat. Res.* **378**, 127–137 (1997).
 49. R. Wiaderkiewicz and A. Ruizcarrillo, Mismatch and blunt to protruding-end joining by DNA ligases. *Nucleic Acids Res.* **15**, 7831–7848 (1987).
 50. L. Chen, K. Trujillo, P. Sung and A. E. Tomkinson, Interactions of the DNA ligase IV-XRCC4 complex with DNA ends and the DNA-dependent protein kinase. *J. Biol. Chem.* **275**, 26196–26205 (2000).
 51. E. B. Cullinan, L. S. Gawron, Y. M. Rustum and T. A. Beerman, Extrachromosomal chromatin—novel target for bleomycin cleavage in cells and solid tumors. *Biochemistry* **30**, 3055–3061 (1991).
 52. O. Tounekti, A. Kenani, N. Foray, S. Orłowski and L. M. Mir, The ratio of single- to double-strand DNA breaks and their absolute values determine cell death pathway. *Br. J. Cancer* **84**, 1272–1279 (2001).
 53. D. Arosio, S. Cui, C. Ortega, M. Chovanec, M. S. Di, G. Baldini, A. Falaschi and A. Vindigni, Studies on the mode of Ku interaction with DNA. *J. Biol. Chem.* **277**, 9741–9748 (2002).
 54. H. Nikjoo, P. O'Neill, M. Terrissol and D. T. Goodhead, Quantitative modelling of DNA damage using Monte Carlo track structure method. *Radiat. Environ. Biophys.* **38**, 31–38 (1999).
 55. H. Nikjoo, R. F. Martin, D. E. Charlton, M. Terrissol, S. Kandaiya and P. Lobachevsky, Modelling of Auger-induced DNA damage by incorporated ^{125}I . *Acta Oncol.* **35**, 849–856 (1996).
 56. X. Y. Gu, R. A. Bennett and L. F. Povirk, End-joining of free radical-mediated DNA double-strand breaks *in vitro* is blocked by the kinase inhibitor wortmannin at a step preceding removal of damaged 3' termini. *J. Biol. Chem.* **271**, 19660–19663 (1996).
 57. R. A. Bennett, X. Y. Gu and L. F. Povirk, Construction of a vector containing a site-specific DNA double-strand break with 3'-phosphoglycolate termini and analysis of the products of end-joining in CV-1 cells. *Int. J. Radiat. Biol.* **70**, 623–636 (1996).
 58. R. B. Painter, B. R. Young and H. J. Burki, Non-repairable strand breaks induced by ^{125}I incorporated into mammalian DNA. *Proc. Natl. Acad. Sci. USA* **71**, 4836–4838 (1974).
 59. R. A. Gibbs, J. Camakaris, G. S. Hodgson and R. F. Martin, Molecular characterization of ^{125}I decay and X-ray-induced HPRT mutants in CHO cells. *Int. J. Radiat. Biol.* **51**, 193–199 (1987).
 60. R. F. Martin and N. Holmes, Use of an ^{125}I -labelled DNA ligand to probe DNA structure. *Nature* **302**, 452–454 (1983).